

# NANO LETTERS

## Letters

---

# High Coverages of Hydrogen on a (10,0) Carbon Nanotube

Charles W. Bauschlicher, Jr.

Mail Stop 230-3, NASA Ames Research Center, Moffett Field, California 94035

Received March 8, 2001 (Revised Manuscript Received April 13, 2001)

### ABSTRACT

The binding energy of H to a (10,0) carbon nanotube is calculated at 24, 50, and 100% coverage using the AM1 and ONIOM approaches. Several different bonding configurations are considered for the 50% coverage case. Using the ONIOM approach, the average C–H bond energy for the most stable 50% coverage and for the 100% coverage are 57.3 and 38.6 kcal/mol, respectively. Considering the size of the bond energy of H<sub>2</sub>, these values suggest that it will be difficult to achieve 100% atomic H coverage on a (10,0) nanotube. The 50% coverage, which appears favorable, corresponds to about 4% by weight storage of H.

**I. Introduction.** Hydrogen storage in carbon nanotubes has attracted much attention recently.<sup>1–4</sup> Claims range from 5–10% by weight at pressures of 1 bar and room temperature<sup>4</sup> to 8.25% by weight at 40 bar and 80 K.<sup>2</sup> Smalley suggested<sup>5</sup> that hydrogen storage could be enhanced, if, in addition to molecular H<sub>2</sub> absorption, atomic hydrogen was

bonded to the walls of the nanotube. We recently<sup>6</sup> computed the binding energy of hydrogen atoms to the side walls of a (10,0) carbon nanotube using the ONIOM method.<sup>7–9</sup> The first C–H bond was 21.6 kcal/mol. The average C–H bond strength for the first two hydrogen atoms was 40.6 kcal/mol and for the first four hydrogens 47.9 kcal/mol. While there

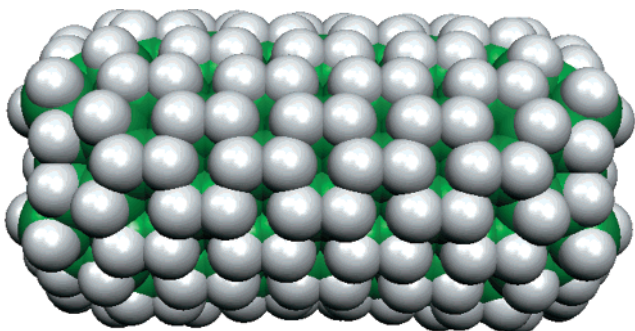


**Figure 1.**  $C_{200}H_{220}$  tube used to model 100% hydrogen coverage on a (10,0) carbon nanotube.

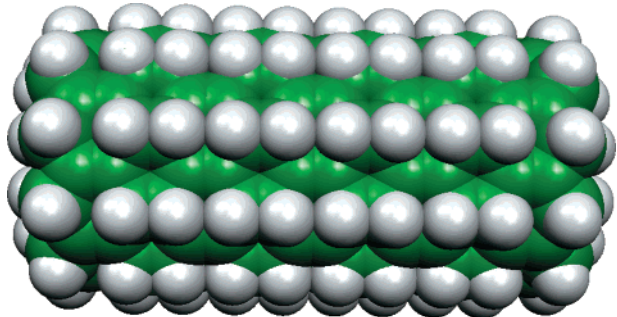


**Figure 2.**  $C_{200}H_{120}$  tube used to model the “lines” form of the 50% hydrogen coverage on a (10,0) carbon nanotube.

is an increase in the bond strength with number of hydrogens, the values were still small compared with the H–H bond at the same level of theory (109.8 kcal/mol). Therefore, we suggested that even at high-hydrogen coverage the C–H bonding would be endothermic or only slightly exothermic. Considering the interest<sup>1–3</sup> in storing H using carbon nanotubes, in this manuscript we report on the results of calculations that model high-H coverages on the same (10,0) carbon nanotube.

**II. Model and Methods.** The initial coordinates of the 20 Å segment of the (10,0) nanotube were generated using the code of Han.<sup>10</sup> The dangling bonds at the ends were tied off with hydrogen atoms, yielding a  $C_{200}H_{20}$  tube. For the 100% coverage, one additional H atom is bound to each carbon atom, thus yielding a  $C_{200}H_{220}$  species, which is shown in Figure 1. For 24% and 50% coverages three random coverage patterns were considered. In each of these, the H atoms were added in pairs. The first H atom was added to one of the bare carbon atoms in a random manner. The second H atom was then added to one of the bare first nearest neighbors in a random manner. If there were no first nearest neighbors, the first H placement was rejected. This approach was used to break individual C–C  $\pi$  bonds and hence maximize the remaining  $\pi$  bonding in the tube.

The observation that F on the outside<sup>11</sup> and I on the inside<sup>12</sup> of carbon nanotubes have distinct patterns, rather than random coverages, leads us to investigate several higher symmetry structures for the 50% H coverage; these cases are shown in Figures 2–6. Figure 2 shows the case where the H atoms are parallel to the axis of the tube and evenly spaced around the tube. In Figure 3, the hydrogens are also along the axis of the tube, but the pairs of lines of H atoms

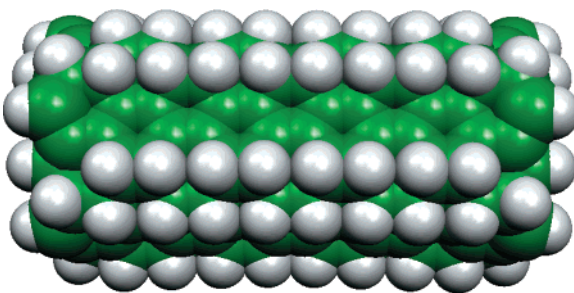


**Figure 3.**  $C_{200}H_{120}$  tube used to model the “pairs of lines” form of the 50% hydrogen coverage on a (10,0) carbon nanotube.

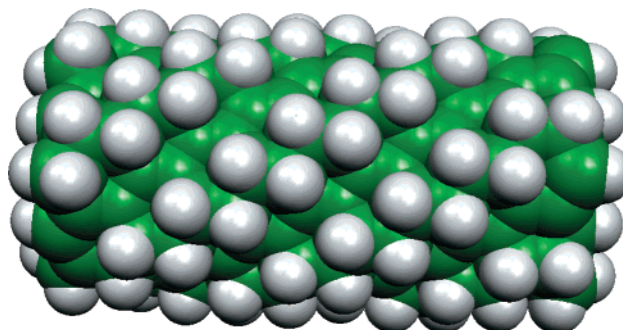


**Figure 4.**  $C_{200}H_{120}$  tube used to model the “spiral” form of the 50% hydrogen coverage on a (10,0) carbon nanotube.

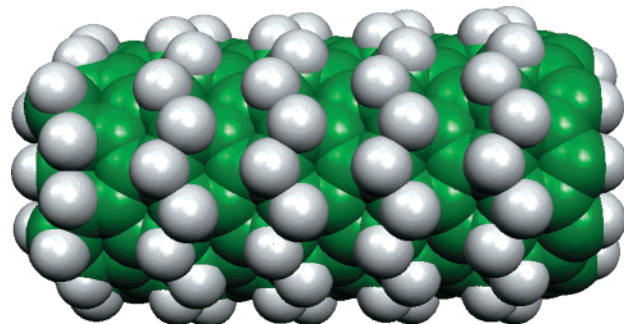


**Figure 5.**  $C_{200}H_{120}$  tube used to model the “rings” form of the 50% hydrogen coverage on a (10,0) carbon nanotube.

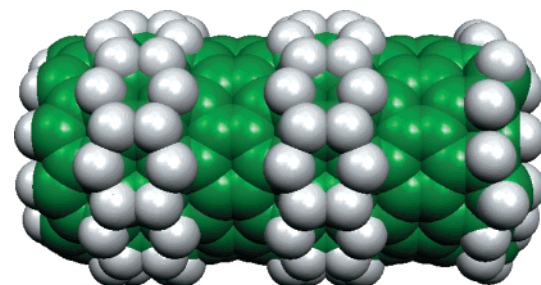


**Figure 6.**  $C_{200}H_{120}$  tube used to model the “pairs of rings” form of the 50% hydrogen coverage on a (10,0) carbon nanotube.

are adjacent. These two structures are denoted “lines” and “pairs of lines”, respectively. In Figure 4, the hydrogens atoms spiral around the tube; this structure is denoted as “spiral”. In Figures 5 and 6, there are rings of H atoms; in the first, denoted “rings”, the hydrogens are evenly spaced, while in the second case, the rings of hydrogen atoms are in pairs, which is denoted as “pairs of rings”.

The AM1 and two-level ONIOM approach<sup>7–9</sup> are used.

**Table 1.** Summary of Hydrogen Binding Energies (kcal/mol)

system	av H binding energy
AM1	
24% random case 1	53.8
24% random case 2	52.1
24% random case 3	48.7
50% random case 1	51.1
50% random case 2	50.7
50% random case 3	48.9
50% pairs of lines	58.3
50% spiral	57.6
50% lines	56.1
50% rings	51.5
50% pairs of rings	48.5
100%	46.8
ONIOM	
1 H <sup>a</sup>	21.6
2 H's <sup>a</sup>	40.6
4 H's <sup>a</sup>	47.9
50% pairs of lines	57.3
50% spiral	52.6
100%	38.7

<sup>a</sup> Taken from ref 6.

The ONIOM approach is a mixed, two-level approach that treats a small section of the system accurately and the rest at a lower level. The present calculations combine the universal force field<sup>13</sup> (UFF), for the low-level treatment, with density functional theory (DFT) for the high-level description. For the DFT, we use the hybrid<sup>14</sup> B3LYP<sup>15</sup> functional. The 4-31G basis set<sup>16</sup> is used in conjunction with the B3LYP calculations. The AM1 calculations are performed using a modified version of Gaussian 94, where damping is used to obtain convergence. ONIOM calculations are performed using Gaussian 98.<sup>17</sup>

The geometries are fully optimized at the AM1 and ONIOM levels of theory. In the ONIOM calculations, 24 carbon atoms, at the center of the nanotube, are used for the high-level treatment. The link hydrogen atoms and the chemisorbed hydrogen atoms are also in the high-level treatment. The atoms included in the high-level treatment are the same as used in our previous treatment<sup>6</sup> of the low-coverage case.

The dangling bonds were terminated with hydrogen atoms to avoid any strain associated with capping the tubes. However, more recent work has shown<sup>18</sup> that capping the carbon nanotubes appears to dramatically speed up the geometry optimization process and, therefore, capping is probably a superior approach, even if it leads to the use of a longer tube.

As noted in our previous study,<sup>6</sup> we encountered problems with local minima for the UFF description of the carbon nanotube, and therefore we use the B3LYP energies instead of the ONIOM energies, since the B3LYP energies were insensitive to the UFF solution. That is, we only use the molecular mechanics approach to constrain the shape of the high-level fragment.

**III. Results and Discussion.** We first consider the results obtained at the AM1 level of theory; see Table 1. The average

H binding energy for three 24% random coverages spans a range of about 5 kcal/mol. Since there are 48 C–H bonds, the stability of the tubes varies by 243 kcal/mol. The average H binding energy for the three random 50% coverages spans a somewhat smaller range, and the values are similar to those obtained for the 24% coverage. We can conclude that the AM1 binding energies for the 24 and 50% coverages are similar, but it would require many more runs to more accurately determine the average bond energies for these two cases and how it changes between them. However, as discussed below, we can get some insight into the bonding using only these few cases.

In light of patterns observed for F and I with nanotubes, rather than consider more random coverages, we studied five higher symmetry patterns, which are shown in Figures 2–6, and their average H binding energies are summarized in Table 1. Three of the higher symmetry structures are more stable than the random coverages. Considering that there are 100 C–H bonds, the change in the average H binding energy means that the three higher symmetry structures are several 100 kcal/mol more stable than the random structures.

The lower stability of the random structures arises for two reasons: (1) there are areas without H atoms that contain an odd number of carbons, which dramatically degrades the  $\pi$  bonding, and (2) to form a good C–H bond, the carbon must  $sp^3$  hybridize, which results in the carbon bulging out of the tube. For the random tubes, there are areas of very high H coverage, and clearly the tube cannot deform such that every atom can form a good  $sp^3$  hybrid bond with H.

For the higher symmetry cases, all regions devoid of H atoms contain an even number of carbon atoms, so the  $\pi$  bonding is not degraded for this reason. For the pairs of lines tube, two rows of carbons bulge out of the tube, allowing the formation of good C–H bonds. This deformation of the carbon tube leaves the bare rows of carbon atoms nearly planar; thus this configuration has both good C–H bonds and good C–C  $\pi$  bonds. In the spiral, the deformation leaves a spiral of good C–H bonds and a spiral of C–C  $\pi$  bonds. In the lines configuration, the geometry appears very favorable for good bonding, but the C–C  $\pi$  bonds are isolated, which removes the  $\pi$  conjugation, and hence this is less favorable than the pairs of lines or spiral. In the two ring forms, the curvature of tube weakens the C–C  $\pi$  bonding, thus these forms are unfavorable, even though they distort to form good C–H bonds.

We studied the two most stable 50% coverage structures, namely, the spiral and pairs of lines, using the ONIOM approach. We computed the average H binding energy of the 12 hydrogens included in the high-level treatment; see Table 1. While we do not compute the H binding energy of the hydrogens in the low-level treatment, their effect on the geometry of the tube is included. The pair of lines ONIOM value is very similar to the AM1 result, while for the spiral, the ONIOM value is somewhat smaller than the AM1 result. On the basis of our low-coverage work, part of the difference between the AM1 and ONIOM values can probably be attributed to the fact that many of the H atoms in the high-level treatment are near the boundary between the high and

low levels of theory. However, it seems unlikely that this can account for the entire difference, and some, if not most, of the difference must be attributed to limitations in the methods used, with the AM1 treatment having a larger uncertainty than the ONIOM approach.

Using the ONIOM approach, we computed the average H binding energy for 100% coverage, and we find that this value is significantly smaller than the 50% coverages. At the AM1 level, the 100% coverage binding energy is also smaller than the 50% cases, but the difference is smaller than found with the ONIOM approach. For the 100% coverage, the carbon atoms still form a good tube structure since any deformation that improves one C–H bond will weaken another. This means that for the 100% coverage the carbons cannot change their hybridization to enhance the C–H bond, which results in a much weaker C–H bond than the 50% coverage, where half of the C atoms can bulge out of the tube to maximize the C–H bonding.

Despite any limitations in the methods used, it is clear that the formation of 100% coverage will be a very endothermic process (remember that the H–H bond energy is 109.8 kcal/mol at this level of theory). The computed binding energies for the 50% coverage cases are sufficiently close to one-half the H–H bond energy that it might be possible to achieve this level of coverage in an exothermic process starting with H<sub>2</sub> and nanotubes. The formation of significantly higher than 50% coverages in an exothermic process seems unlikely since higher coverages would require a deformation of the carbons in the tube that would weaken some of the existing C–H bonds and hence result in a smaller average H binding energy. The 50% coverage corresponds to only about 4% by weight.

It should be noted that all of our discussion is for the case of H atoms on the outside of the tube. It might be possible to achieve high coverage by bonding some H atoms on the inside of the tube and some on the outside. For example, one-half the C atoms bulge out and bond to H atoms and the other half of the C atoms bulge in and bond to H atoms on the inside of the tube. However, this approach faces the problem of opening the tubes and getting an H atom inside.

For F on an (18,0) tube, Kudin et al.<sup>19</sup> found the spiral structure to be more stable than the lines form, and both were more stable than ring structures. Thus, their fluorine results are similar to our hydrogen results. For fluorine, it would be very interesting to know the stability of the pairs of lines form relative to the other forms. Froudakis<sup>20</sup> found a ring structure to be more favorable than a line structure for hydrogen on a (4,4) tube. Clearly, more work on the coverage patterns as a function of type of tube is required.

**IV. Conclusions.** We use the AM1 level of theory to obtain some insight into the bonding of H atoms to a (10,0) carbon nanotube. The carbon atoms that bond to the H atoms bulge out of the tube to improve the sp<sup>3</sup> hybridization, which enhances the C–H bond. For 50% coverage we have found two structures that have half of the C atoms bulged out of the tube to form good C–H bonds, while the remaining carbons atoms can still have good  $\pi$  bonding. Random coverages are found to be much less favorable because not all atoms have a favorable orientation for either C–H or C–C  $\pi$  bonding. Random coverage also tends to lead to bare regions with an odd number of carbon atoms, which is not ideal for  $\pi$  bonding. Using the ONIOM approach, the average C–H bond energy was computed for the two most favorable 50% coverage cases as well as for 100% coverage. It is possible that the formation of 50% coverage is thermodynamically favorable, but it is concluded that the formation of 100% coverage will be very endothermic.

## References

- Chen, P.; Wu, X.; Lin, J.; Tan, K. L. *Science* **1999**, 285, 91.
- Ye, Y.; Ahn, C. C.; Witham, C.; Fultz, B.; Liu, J.; Rinzler, A. G.; Colbert, D.; Smith, K. A.; Smalley, R. E. *Appl. Phys. Lett.* **1999**, 74, 2307.
- Simonyan, V. V.; Diep, P.; Johnson, J. K. *J. Chem. Phys.* **1999**, 111, 9778.
- Dillon, A. C.; Jones, K. M.; Bekkedahl, T. A.; Kaing, C. H.; Behmune, D. S.; Heben, M. J. *Nature* **1997**, 386, 377.
- Smalley, R. E. Personal communication.
- Bauschlicher, C. W. *Chem. Phys. Lett.* **2000**, 322, 237.
- Svensson, M.; Humbel, S.; Froese, R. D. J.; Matsubara, T.; Sieber, S.; Morokuma, K. *J. Phys. Chem.* **1996**, 100, 19357.
- Humbel, S.; Sieber, S.; Morokuma, K. *J. Chem. Phys.* **1996**, 105, 1959.
- Maseras, F.; Morokuma, K. *J. Comput. Chem.* **1995**, 16, 1170.
- Han, J. Personal communication.
- Kelly, K. F.; Chiang, I. W.; Mickelson, E. T.; Hauge, R. H.; Margrave, J. L.; Wang, X.; Scuseria, G. E.; Radloff, C.; Halas, N. J. *Chem. Phys. Lett.* **1999**, 313, 445.
- Fan, X.; Dickey, E. C.; Eklund, P. C.; Williams, K. A.; Grigorian, L.; Buczko, R.; Pantelides, S. T.; Pennycook, S. J. *Phys. Rev. Lett.* **2000**, 84, 4621.
- Rappe, A. K.; Casewit, C. J.; Colwell, K. S.; Goddard, W. A.; Skiff, W. M. *J. Am. Chem. Soc.* **1992**, 114, 10024.
- Becke, A. D. *J. Chem. Phys.* **1993**, 98, 5648.
- Stephens, P. J.; Devlin, F. J.; Chabalowski, C. F.; Frisch, M. J. *J. Phys. Chem.* **1994**, 98, 11623.
- Frisch, M. J.; Pople, J. A.; Binkley, J. S. *J. Chem. Phys.* **1984**, 80, 3265 and references therein.
- Frisch, M. J.; et al. *Gaussian* 98, revision A.7; Gaussian, Inc.: Pittsburgh, PA, 1998.
- Bauschlicher, C. W. Unpublished.
- Kudin, K. N.; Bettinger, H. F.; Scuseria, G. E. *Phys. Rev. B* **2001**, 63, 045413.
- Froudakis, G. E. Preprint communicated to this author.

NL010018N